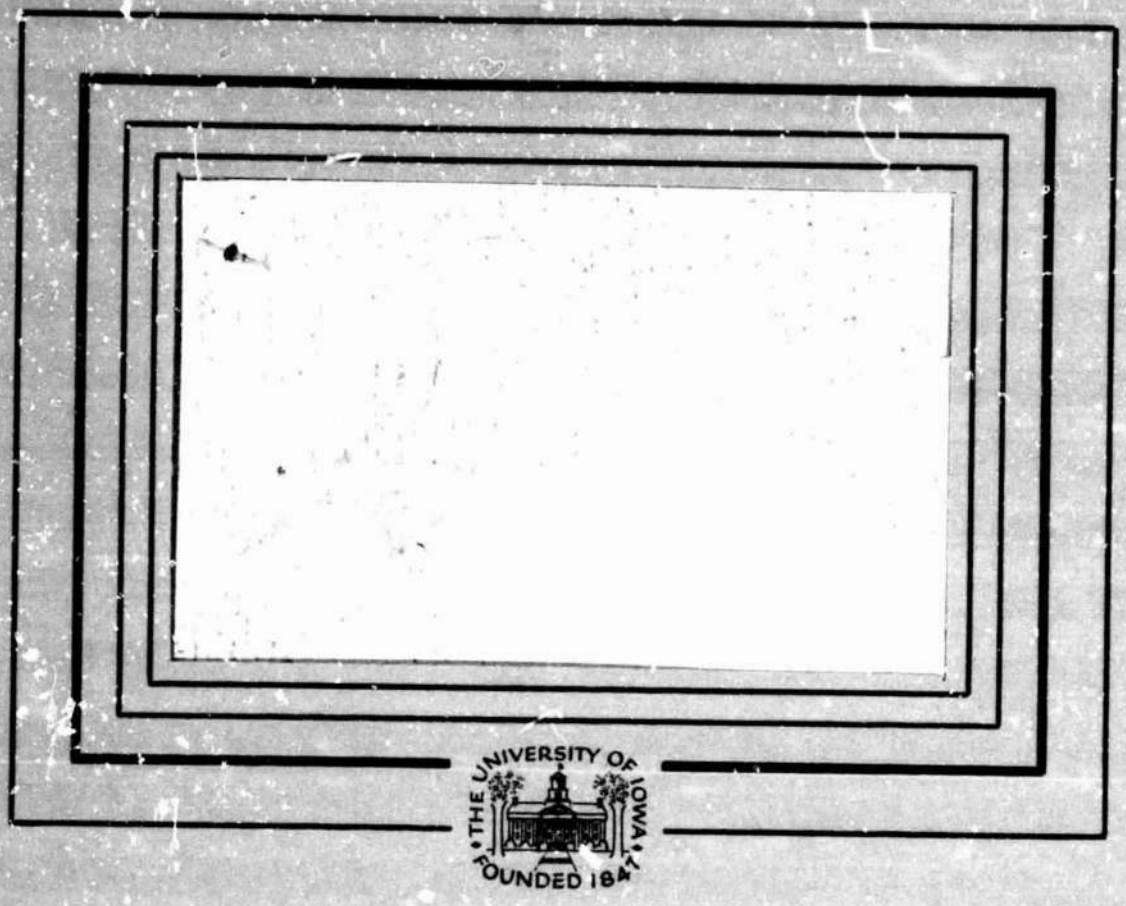

Department of Physics and Astronomy

THE UNIVERSITY OF IOWA

Iowa City, Iowa 52242

THE TEMPORAL EVOLUTION OF A SMALL AURORAL SUBSTORM AS VIEWED FROM HIGH ALTITUDES WITH DYNAMICS EXPLORER 1

by

J. D. Craven and L. A. Frank

January 1985

Department of Physics and Astronomy
The University of Iowa
Iowa City, Iowa 52242

ABSTRACT

A small auroral substorm is investigated with auroral imaging photometers carried on the spacecraft Dynamics Explorer 1. Initial brightening along the auroral oval and the subsequent westward and poleward motions of intense, localized emission regions are associated with auroral surges. Following substorm onset, another region of less intense emissions is observed to develop at lower latitudes and adjacent to the bright region near local midnight. This second region expands towards the east. The bright zone of auroral emissions associated with the surges is interpreted as the signature of electron acceleration along magnetic field lines threading the boundary layer of the plasma sheet in the magnetotail. The more diffuse, less intense region is identified with eastward-drifting electrons injected into the plasma sheet and ring current following substorm onset. No rapid poleward motion of the discrete aurora is detected during substorm recovery.

INTRODUCTION

A principal objective of global imaging with Dynamics Explorer 1 (DE 1) is to observe the dramatic variations in spatial distributions and intensities of auroral luminosities during substorms. The present model of a substorm [see Akasofu, 1964, 1977] is based in large part on observations with ground-based, all-sky cameras and imaging instruments on low-altitude spacecraft. All-sky cameras provide good temporal resolution (1 min) over limited areas (800-km diam), while low-altitude spacecraft provide a nearly global view of the auroral oval during a ~ 15-minute traversal of the polar latitudes which cannot be repeated during a typical auroral substorm. With DE 1, images of the entire auroral oval can be telemetered at a rate of five per hour from each of three imaging photometers for continuous periods of 4-5 hours in each orbit. Thus, an entire substorm can be continuously monitored. In this report we present an analysis of a small substorm which is qualitatively representative of numerous small substorms observed with the DE-1 auroral imagers. Descriptions of the three imaging photometers are given by Frank et al. [1981a].

OBSERVATIONS

A typical, small auroral substorm observed in the light of atomic oxygen (OI) at 557.7 nm is shown in the 12 consecutive images of Plate 1. The observing period is 28 November 1981 from 1333 to 1559 UT as DE 1 proceeds across the northern polar region from the morning sector of local time near apogee (3.65 R_E altitude) to the evening sector at an altitude of 1.9 R_E. The orbital plane bisects each image vertically. The images are processed to remove contributions from atmospheric dayglow and are overlayed with the surface limb and the line of constant solar zenith angle equal to 98°. The color bar for this false-color presentation extends from ~ 1 kilorayleigh (light blue) to ~ 55 kR (white).

The first three images record the brief brightening of a discrete auroral form in the midnight sector to ~ 22 kR. This is followed by a second, sustained increase beginning at ~ 1410 UT (fourth image), which is the substorm of interest here. Maximum intensities $\gtrsim$ 40 kR are detected from 1434 to 1458 UT (sixth and seventh images) as the longitudinal and latitudinal widths of the auroral features increase significantly. The time history of maximum intensities observed by the two visible-wavelength photometers (A and B) is presented in the upper panel of Figure 1. The duration of the substorm is ~ 1.3 hours. Magnetometers at Dixon Island and Tixie Bay record variations in the H and Z components with magnitudes of ~ 50-80 nT (data courtesy of S.-I. Akasofu).

Motions of the poleward and equatorward boundaries of the aurora at the 4-kR level are displayed in Figure 2, along with contours of constant invariant latitude $\Lambda = 65°$ and 75°. Geographic polar coordinates are used. To provide uniform sampling in time across the auroral oval for the mode of operation employed during this period, the first, third ... (second, fourth ...) diagrams are derived from images gained with the A (B) photometer. The second diagram is obtained from the fourth image of Plate 1. The UT for each diagram corresponds to that for the sampling of the aurora at local midnight. Little structure is observed for the early portion of the substorm (1405 to 1429 UT) as the discrete auroral form expands rapidly in longitude and shifts in position towards the late-evening sector. As the substorm develops further, the pattern of auroral emissions begins to expand steadily into the morning sector, not from the latitude of the eastern edge of the initial discrete aurora, but from its equatorward edge near local midnight. Motion of the discrete auroral form is seen to proceed into the evening sector from the latitude of the existing aurora. Hence, we are able to observe directly the temporal development of the aurora which gives rise to the 'distinct differences in the characteristics of auroras between the evening and morning sectors' observed in DMSP photographs [Akasofu, 1977, p. 78].

The longitudes for the eastward and westward extents of the 4-kR boundary are shown in Figure 1b for the period 1330 to 1600 UT. The longitude for the maximum intensity in each image is also given. The longitudinal width is initially very small, expands briefly to ~ 40° with the brightening at ~ 1345 UT, and again contracts. After 1408 UT the width increases rapidly as maximum

auroral intensities increase to ~ 1[illegible] kR. This initial expansion to a longitudinal width of ~ 90° at 1418 UT is followed by a significant westward motion of the eastward contour by ~ 40° during the interval 1418 to 1428 UT. The expansion rate in the evening sector remains rapid and westward, at -292°/hour, or ~ 3600 m/s. During this 10-minute period maximum auroral intensities increase to ~ 25 kR. Throughout the remainder of the substorm, the westward and eastward edges of the aurora expand at steady rates into the evening and morning sectors. Least-squares fits yield rates of -26.7° and +45.0°/hour in the rotating frame of a terrestrial observer, or ~ 330 and ~ 550 m/s, respectively.

Prior to 1418 UT the relatively weak maxima appear progressively at more easterly locations along the auroral oval. After ~ 1418 UT, in the early phase of the substorm, the motion of the maxima shifts abruptly westward and then proceeds more slowly in a westerly direction for the remainder of the event. A least-squares yields a westward rate of -49.1°/hour, or ~ 600 m/s, after 1426 UT. Analysis of consecutive images reveals that the site at which a maximum in intensities is first detected experiences a brightening to its maximum emission intensities followed by a decrease in intensities. The next maximum is associated with increasing intensities at a new location. The apparent westward motion is due to the sequential appearance of new maxima and not to the steady motion of a few bright features.

Latitudinal motion of the 4-kR poleward boundary of the aurora at 120° E longitude (~ 23 hours local time) proceeds steadily from a corrected geomagnetic latitude of 67.7° ($\Lambda \approx 67°$) near onset of the substorm at 1415 UT to 72.1° ($\Lambda \approx 71°$) by 1450 UT, as shown in the lower panel of Figure 1.

A gradual increase of ~ 1° occurs in the next hour. We do not observe the ~ 5° 'poleward leap' in latitude for the longitudinally extended discrete aurora in the pre-midnight sector anticipated by Pytte et al. [1978] and expected to occur early in the recovery phase.

The spatial distribution of the aurora at 1510 UT following the maximum epoch of the substorm is displayed more clearly in Plate 2 by expanding the ninth (lower-left) image of Plate 1 and by a summary diagram in Figure 3. Additional information concerning the distribution of auroras around the oval is provided at $\lesssim$ 1 kR with the two visible-wavelength photometers and by images gained simultaneously at vacuum-ultraviolet wavelengths (not shown). A weak auroral arc (< 1 kR) extends from the poleward edge of the intense discrete aurora near midnight into the morning sector at polar-cap latitudes. This weak polar-cap arc is not detected in later images. Near midnight, discrete features are observed to reorient in a more equatorward direction as they 'blend' into the less intense auroral region to the east at lower latitudes.

DISCUSSION

We associate changes in position of the intense luminous features in the pre-midnight sector with the westward and poleward episodic motion of surges in the auroral electrojet described by Wiens and Rostoker [1975]. In contrast to westward propogation speeds of ~ 2000 m/s observed by Wiens and Rostoker (see their Figures 12, 17 and 20), speeds for this small substorm are ~ 600 m/s following a brief (~ 10 min) westward motion at ~ 3600 m/s. As peak emission intensities of ~ 50 kR are approached in the pre-midnight sector, less intense (~ 10-15 kR), more diffuse auroral forms appear and then expand eastward from near local midnight at more equatorward latitudes. We associate these post-midnight auroral features with the patchy and diffuse auroral forms observed during recovery phases of substorms [e.g., Akasofu, 1964]. The decrease in peak intensities for the discrete auroral forms in the pre-midnight sector is followed within ~ 30 minutes by a decrease in the intensities of the eastward moving auroral forms within the post-midnight sector. Additionally, the decrease in the intensities of the diffuse aurora appears to be greatest near midnight, resulting in a separation between the two auroral emission regions.

Our interpretation of these observations is based upon the idea that the discrete aurora maps to the plasma-sheet boundary layer [e.g., Frank et al., 1981b; Eastman et al., 1984; Lyons and Evans, 1984]. The bright areas of intense aurora emissions in the pre-midnight sector are further interpreted as signatures of the distant source region in the magnetotail for plasma acceleration and heating, and which drives field-aligned and ionospheric currents associated with the discrete aurora and the surge. This region is distinct

from the acceleration region at low altitudes (1-2 R_E) responsible for the monoenergetic peak in electron spectra observed above the aurora.

Note that the longitudinal width here of the discrete aurora is $\lesssim 50°$, and is confined to the pre-midnight sector. Extension of the plasma-sheet boundary layer into the post-midnight sector might then be identified with the solitary discrete polar feature noted here. The DMSP image shown as Figure 1 by Baumjohann and Opgenoorth [1984] provides a higher-resolution view of the principal spatial features identified here, but without coverage of the temporal evolution of these auroral features.

The temporal development of intense discrete auroral forms is followed by the appearance of a region of diffuse emissions. The first appearance of the diffuse region near the east and equatorward edge of the more intense discrete auroral forms suggests that electrons from the distant acceleration region and along the plasma-sheet boundary layer are injected into the lower-latitude region of the magnetotail to enhance the plasma sheet and ring current, and drift eastward in response to gradients and curvature in the magnetic field. Pitch-angle scattering of these eastward-drifting electrons to atmospheric altitudes is then responsible for the diffuse auroral forms in the post-midnight sector.

ACKNOWLEDGEMENTS

This research was supported in part by the National Aeronautics and Space Administration under contract NAS5-25689 and grants NGL-16-001-002 and NAG5-483, and by the Office of Naval Research under grant N00014-76-C-0016.

REFERENCES

Akasofu, S.-I., The development of the auroral substorm, Planet. Space Sci., 12, 273-282, 1964.

Akasofu, S.-I., Physics of Magnetospheric Substorms, D. Reidel, Dordrecht, Netherlands, 1977.

Baumjohann, W. and H. J. Opgenoorth, Electric fields and currents associated with active aurora, in Magnetospheric Currents, ed. by T. A. Potemra, AGU Geophysical Monograph 28, 1984.

Eastman, T. E., L. A. Frank, W. K. Peterson and W. Lennartsson, The plasma sheet boundary layer, J. Geophys. Res., 89, 1553-1582, 1984.

Frank, L. A., J. D. Craven, K. L. Ackerson, M. R. English, R. H. Eather and R. L. Carovillano, Global auroral imaging instrumentation for the Dynamics Explorer Mission, Sp. Sci. Instr., 5, 369-393, 1981a.

Frank, L. A., R. L. McPherron, R. J. DeCoster, B. G. Burek, K. L. Ackerson and C. T. Russell, Field-aligned currents in the Earth's magnetotail, J. Geophys. Res., 86, 687-700, 1981b.

Lyons, L. R. and D. S. Evans, An association between discrete aurora and energetic particle boundaries, J. Geophys. Res., 89, 2395-2400, 1984.

Pytte, T., R. L. McPherron, M. G. Kivelson, H. I. West, Jr. and E. W. Hones, Jr., Multiple-satellite studies of magnetospheric substorms: plasma sheet recovery and the poleward leap of auroral zone activity, J. Geophys. Res., 83, 5256-5268, 1978.

Wiens, R. G. and G. Rostoker, Characteristics of the development of the westward electrojet during the expansive phase of magnetospheric substorms, J. Geophys. Res., 80, 2109-2128, 1975.

PLATE CAPTIONS

Plate 1. Twelve consecutive images of the northern auroral oval for emissions of atomic oxygen (OI) at 557.7 nm from 1333 to 1559 UT on 28 November 1981. Time increases left to right, top to bottom. The first three image frames record the brief brightening of a discrete auroral form at local midnight. The substorm discussed here is observed beginning with the fourth frame at 1410 UT. These images are obtained with Photometer B.

Plate 2. Expanded view of the ninth (lower-left) image of Plate 1 obtained during the 12-minute interval 1510 to 1523 UT. Contours of constant invariant latitude Λ = 65° and 75° are overlayed on the image in the dark hemisphere. The line of constant solar zenith angle at 98° delineates the position at which the auroral emissions at 557.7 nm can be separated from the sunlit upper atmosphere.

FIGURE CAPTIONS

Figure 1. (a) Maximum intensities of the discrete aurora in the region of the westward traveling surge for OI emissions at 557.7 nm during the period 1337 to 1544 UT. (b) Geographic longitudes of the eastward and westward edges of 4-kR intensity contours. Also shown are the positions of intensity maxima within the surge region as they progress westward. (c) Corrected geomagnetic latitudes of the poleward and equatorward edges of the auroral oval at 120° E longitude (~ 23 hours local time) for intensities $\geq$ 4 kR.

Figure 2. The 4-kR intensity contours for nine consecutive images, displayed in geographic polar coordinates. Contours of constant Λ = 65° and 75° are also given. The Universal Times corresponding to the measurements of auroral intensities at local midnight are indicated for each image.

Figure 3. Summary diagram for the image of Plate 2 to identify the two auroral emission regions.

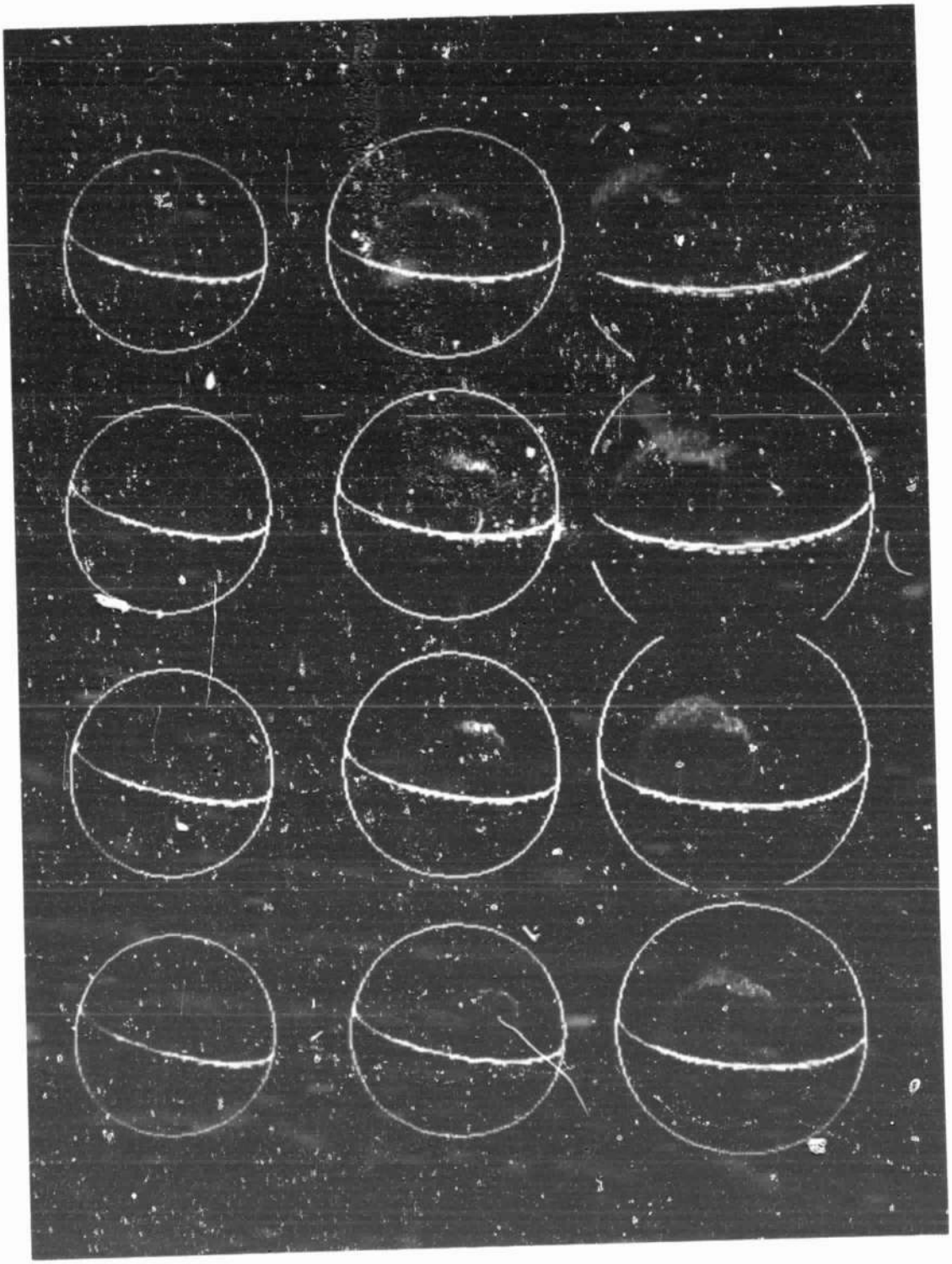

Plate 1

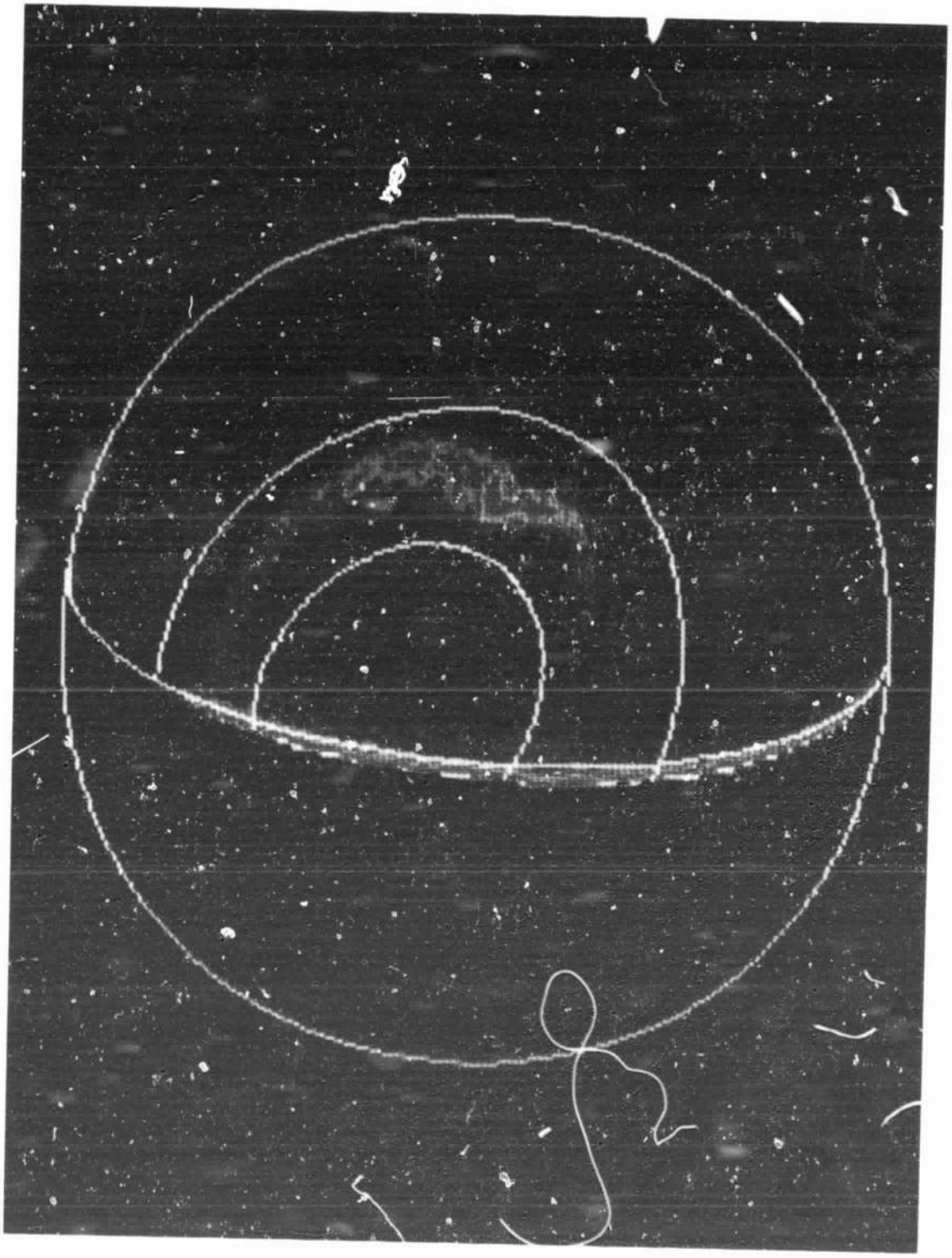

Plate 2

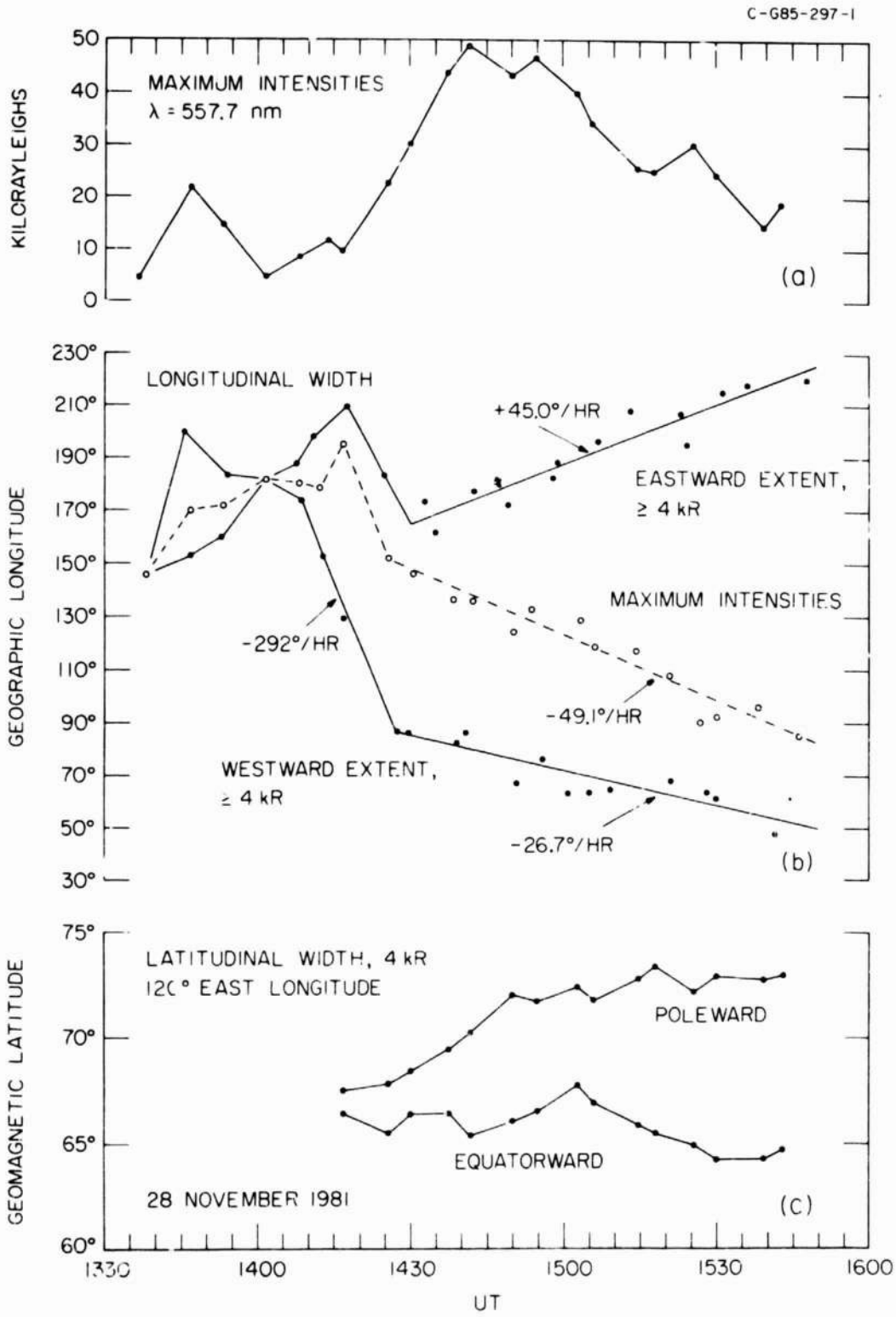
C-G85-297-1
KILORAYLEIGHS
MAXIMUM INTENSITIES
λ = 557.7 nm
(a)
GEOGRAPHIC LONGITUDE
LONGITUDINAL WIDTH
+45.0°/HR
EASTWARD EXTENT,
≥ 4 kR
MAXIMUM INTENSITIES
-292°/HR
-49.1°/HR
WESTWARD EXTENT,
≥ 4 kR
-26.7°/HR
(b)
GEOMAGNETIC LATITUDE
LATITUDINAL WIDTH, 4 kR
120° EAST LONGITUDE
POLEWARD
EQUATORWARD
28 NOVEMBER 1981
(C)
UT

Figure 1

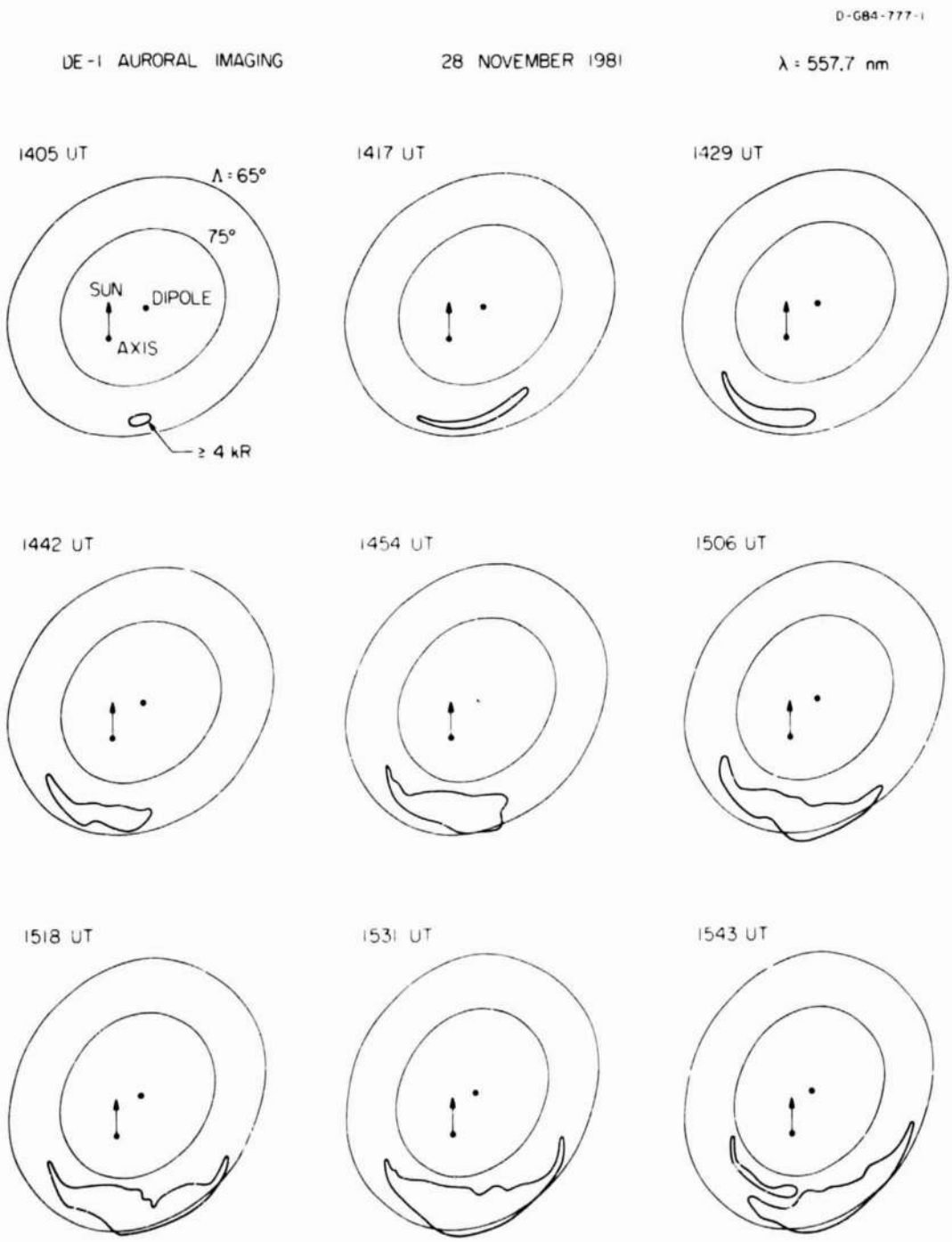
DE-1 AURORAL IMAGING
28 NOVEMBER 1981
λ = 557.7 nm
1405 UT
Λ = 65°
75°
SUN
DIPOLE
AXIS
≥ 4 kR
1417 UT
1429 UT
1442 UT
1454 UT
1506 UT
1518 UT
1531 UT
1543 UT

Figure 2

C-G84-781-I

POLAR VIEW OF THE AURORAL OVAL

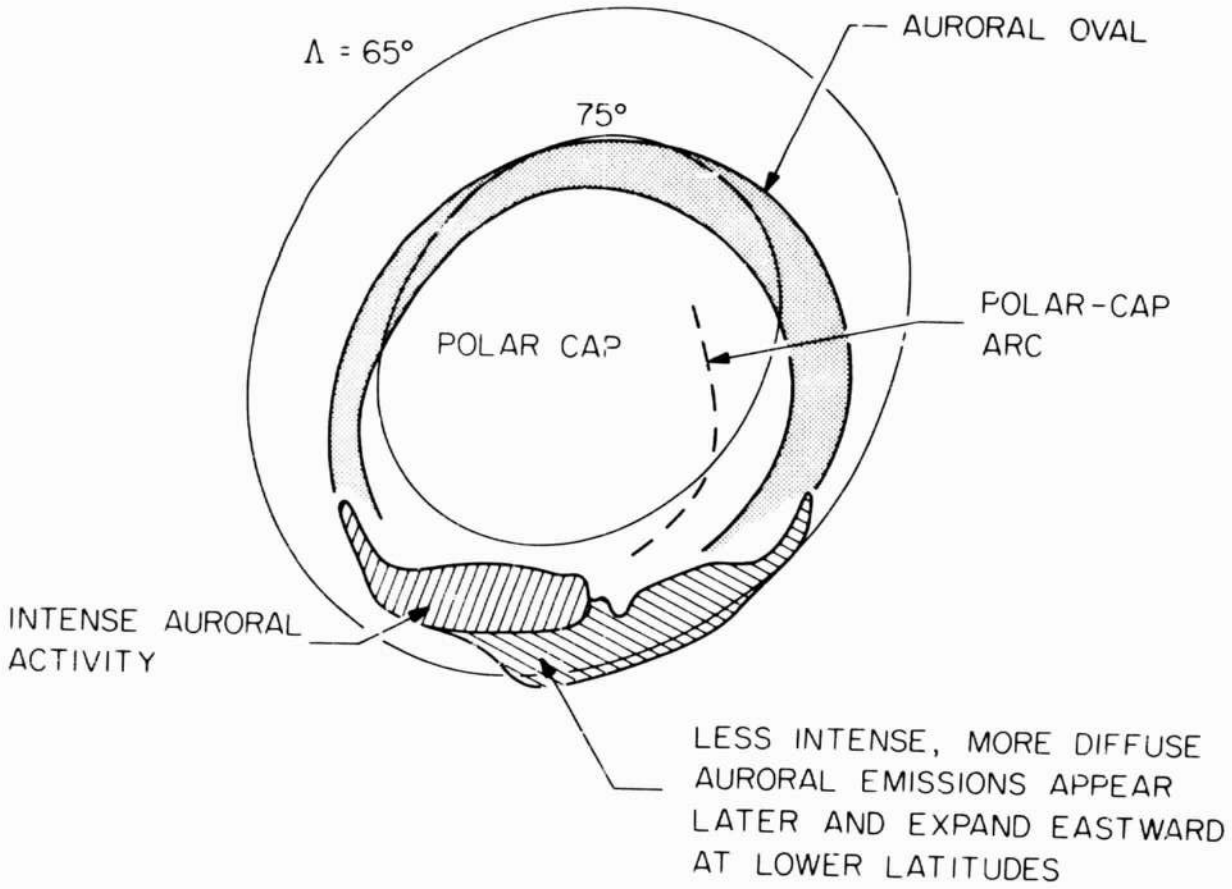

Figure 3